ON THE THREE-DIMENSIONAL COLLISION PROBABILITIES RELEVANT TO ATM

L.M.B.C. Campos[1,2], J.M.G. Marques[1,3]
[1]Centro de Ciências e Tecnologias Aeronáuticas e Espaciais.
[2]Instituto Superior Técnico, Av. Rovisco Pais, 1049-001, Lisbon, Portugal.
[3]Universidade Lusófona de Humanidades e Tecnologias,
Av. Campo Grande, 376, 1749-024, Lisbon, Portugal. jmgmarques@ulusofona.pt

Keywords: *Aircraft Separation, Safety Metrics, Collision Probabilities.*

Abstract

The separation of aircraft in cruising flight in air corridors is based on reducing the risk of collision due to position inaccuracy caused by navigation errors, atmospheric disturbances or other factors. The appropriate standard is the International Civil Aviation Organization Target Level of Safety of less than 5×10^{-9} *per flight hour. An upper bound for the collision probability per unit distance is the probability of coincidence, in the case of aircraft flying in parallel tracks in the same direction. This leads to the case of two aircraft flying at a constant separation, for which at least three probabilities of coincidence can be calculated: (i) the maximum probability of coincidence, at the most likely point; (ii) the cumulative probability of coincidence, integrated along the flight path; (iii) the cumulative probability of coincidence integrated over all space. These three probabilities of coincidence are applied to the old standard and new reduced vertical separations of* 2000 ft *and* 1000 ft *respectively, for comparison with the ICAO TLS, and also to assess their suitability as safety metrics. The results are found to be sensitive to the choice of probability distribution. Also several alternative safety metrics are considered.*

1 Introduction

The growth in air transport requires increasing air traffic capacity without degrading safety [1-3]. Air traffic capacity is determined by aircraft separation. The latter is influenced by two types of criteria: (i) the wake vortex effects, e.g. for aircraft on approach to land [4-8]; (ii) the position errors, e.g. lateral or vertical, which can lead to collisions. The present paper addresses only the latter (ii) aspect; a simple safety criterion is the International Civil Aviation Organization (ICAO) [4] Target Level of Safety (TLS) specifying a probability of collision less than 5×10^{-9} per hour. A specified level of safety should be achievable by setting separation rules [5] and specifying a corresponding navigation accuracy [6,7]; a final safety net is provided by conflict resolution methods [8], or equipment like T-CAS. The models of collision probabilities [9-17] usually do not involve aircraft dynamics or atmospheric disturbances [18-22] nor stability of flight aspects [23-27]; the implication is that the navigation errors, atmospheric disturbances or flight manouevers, or their combination is such that the position error satisfies a given probability distribution [28-35]. Thus the choice of a probability distribution becomes the critical element to calculate collision probabilities, and thereby assess safety of Air Traffic Management (ATM). The Gaussian probability distribution [28] is widely used, because of the central limit theorem of the statistics. In addition, the central limit theorem depends on the satisfaction of Linderberg´s condition [29], requiring that events which large deviation from the mean make a small contribution to the variance; this condition is not directly related to the fact that it is precisely the large deviations which pose the greatest collision risk. Hence the main objection to the use of the central limit theorem may not be the Lindeberg condition, but is certainly the failure of the law of large numbers.

The statistics of collisions, like other rare events [30], corresponds to the tail of the probability distribution [31]. It was been known for a long time that the Gaussian underestimates the probability of collision, and among the simplest probability distributions the Laplace distribution is a better choice [9]. Both the Gaussian and Laplace distributions are particular cases [31] of the generalized error (or Laplace) distribution, which has been shown to model the tail and or large flight path deviations obtained from radar tracks [10,12,14]; the modeling of both the core and tail, i.e. the full range of flight path deviations from small to large can be done by further extension to the combined Gamma and generalized error probability distribution [32]; the latter can be asymmetric relative to the mean value [33-35], e.g. for a crossing of climbing and descending aircraft [36] the probabilities may be different for altitude gain or loss. For the purpose of safety assessment, the collision probability may be replaced by an upper bound which is easier to estimate [37]. The probability of collision can be specified [9] as the probability of penetration of the safety volumes around each aircraft; it is not necessary to discuss here the details of the safety volume, because it can be replaced in the case of aircraft flying on parallel paths, by an upper bound [15] which is the probability of coincidence.

In the present paper the case of two aircraft on the parallel tracks with a vertical separation L_z taken as example (*Figure 1*). The probability of deviations from the flight path is in the first instance assumed to satisfy a Gaussian distribution [28]; the Laplace distribution has also been used [9], and the generalized error distribution [10-15] is a more accurate alternative. The accuracy of the generalized error distribution as a representation large flight path deviations has been shown with reference to aircraft radar tracks [10-15]. The maximum probability of coincidence, at the point of most likely coincidence (§2), leads to a probability per square nautical mile flown; the probabilities of coincidence are less at the other positions across the flight path, but non-negligible, and three-dimensional integration over all space leads (§3) to a cumulative probability of collision in units of distance flown. If the integration is made in one dimension across the flight path, the cumulative probability of coincidence appears per unit distance (§4). The latter, when multiplied by the aircraft velocity, leads to a probability per unit time, which can be compared (§5) with the ICAO TLS standard. These various measures of probability of coincidence as a function of separation distance L and the r.m.s. position errors σ_1 and σ_2 of the two aircraft lead to safety metrics [1], which can be used in the analysis of flight data or results of real or fast time simulations.

2 Maximum probability of coincidence for dissimilar aircraft

Consider (*Figure 1*) two aircraft flying along the same straight flight path at a minimum separation distance L. It is assumed, for convenience of calculation, that the position errors satisfy Gaussian statistics [5], although Laplace [3] or other statistics [4,6] could be used. The Gaussian probability that the first aircraft deviates a distance r_1 from its intended position is:

$$P_1(\vec{r}_1) = \left[1/\left(\sigma_1\sqrt{2\pi}\right)\right]\exp\left[-\left(|\vec{r}_1|/\sigma_1\right)^2/2\right], \tag{1a}$$

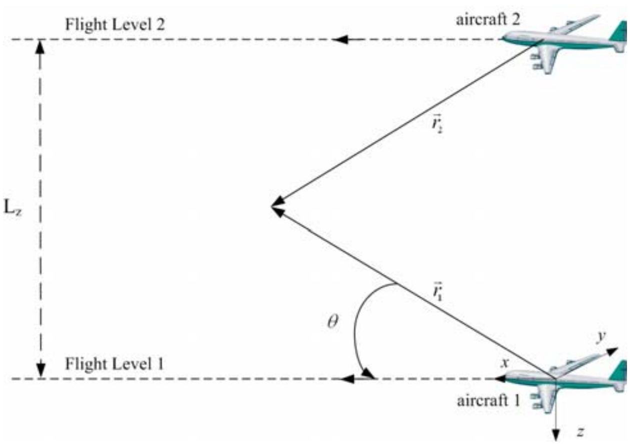

Fig. 1 - Two aircraft flying along the same straight flight path at minimum separation distance, with the first having a position drift $\mathbf{r}_1$ and the second a position drift $\mathbf{r}_2$ leading to a coincidence anywhere in three dimensions.

where σ_1 is the r.m.s. position error; using spherical coordinates (r, θ, ϕ) with origin on aircraft 1, and polar axis along the flight path, the position vector $\vec{r}_1$ of the deviation of the first aircraft has Cartesian components:

$$\vec{r}_1 = r\left(\cos\theta, \sin\theta\cos\phi, \sin\theta\sin\phi\right). \tag{1b}$$

The second aircraft may have a distinct r.m.s. position error σ_2, corresponding to a probability of deviation to a position $\vec{r}_2$:

$$P_2\left(\vec{r}_2\right) = \left\{1/\left[\sigma_2\sqrt{2\pi}\right]\right\}\exp\left[-\left(\left|\vec{r}_2\right|/\sigma_2\right)^2/2\right], \tag{2a}$$

where a coincidence occurs if:

$$\vec{r}_2 = \left(L - r\cos\phi, r\sin\theta\cos\theta, r\sin\theta\sin\phi\right), \tag{2b}$$

using a spherical coordinate system centred on the first aircraft with polar axis along the flight path. Here the size of the aircraft is omitted, by including it [4] either in the separation L or in the r.m.s. position errors σ_1 and σ_2. Assuming that the position errors of the two aircraft are statistically independent, the probability of coincidence is the product of (1a) and (2a):

$$P_{12}\left(r,\theta\right) = P_1\left(\vec{r}_1\right) \; P_2\left(\vec{r}_2\right), \tag{3}$$

where

$$P_1\left(\vec{r}_1\right) = \left[1/\left(\sigma_1\sqrt{2\pi}\right)\right] \; \exp\left[-\left(r/\sigma_1\right)^2/2\right], \tag{4a}$$

$$P_2\left(\vec{r}_2\right) = \left[1/\left(\sigma_2\sqrt{2\pi}\right)\right] \times\exp\left\{-\left(r^2 + L^2 - 2rL\cos\theta\right)/\left[2\left(\sigma_2\right)^2\right]\right\}. \tag{4b}$$

The radius r appears in both expressions, the polar angle θ only in (4b), and the azimuthal angle ϕ not at all, because the probability of coincidence is axially symmetric.

From (3; 4a,b) the probability of coincidence depends on the position (r, θ):

$$P_{12}\left(r,\theta\right) = \left[1/\left(2\pi\sigma_1\sigma_2\right)\right] \; \exp\left[-\left(L/\sigma_2\right)^2/2\right] \times\exp\left\{-\left(r^2/2\right)\left[\left(\sigma_1\right)^{-2} + \left(\sigma_2\right)^{-2}\right] + rL\left(\sigma_2\right)^{-2}\cos\theta\right\}. \tag{5}$$

Its extremum is specified by the first derivatives:

$$\partial P_{12}\left(r,\theta\right)/\partial\theta = -P_{12}\left(r,\theta\right) rL\left(\sigma_2\right)^{-2}\sin\theta, \tag{6a}$$

$$\partial P_{12}\left(r,\theta\right)/\partial r = P_{12}\left(r,\theta\right) \times\left\{-r\left[\left(\sigma_1\right)^{-2} + \left(\sigma_2\right)^{-2}\right] + L\left(\sigma_2\right)^{-2}\cos\theta\right\}. \tag{6b}$$

The extremum of the probability of coincidence occurs when both derivatives vanish:

$$\partial P_{12}\left(r_m,\theta_m\right)/\partial r = 0 = \partial P_{12}\left(r_m,\theta_m\right)/\partial\theta, \tag{7a,b}$$

which is the case on the flight path (8a):

$$\theta_m = \pi, \quad r_m/L = 1/\left[1 + \left(\sigma_2/\sigma_1\right)^2\right], \tag{8a,b}$$

at the position (8b), *viz.*: (i) for aircraft with equal r.m.s. position errors $\sigma_1 = \sigma_2$ the maximum probability of coincidence is at a position $r_m = L/2$ half-way between them; (ii) for aircraft with unequal r.m.s. position errors $\sigma_2 \neq \sigma_1$ the maximum probability of coincidence occurs at a position closer to the aircraft which has more 'accurate' navigation because it is the less accurately navigating aircraft which deviates most, viz. $r_m < L/2$ for if $\sigma_1 > \sigma_2$ and $r_m < L/2$ if $\sigma_1 < \sigma_2$.

In order to prove that the extremum (8a,b) in the probability of coincidence (5) is actually a maximum (and not a minimum, or an inflexion), it is necessary to consider second-order derivatives, i.e. one order beyond (6a,b), *viz.*:

$$\partial^2 P_{12}\left(r,\theta\right)/\partial\theta^2 = -P_{12}\left(r,\theta\right) rL\left(\sigma_2\right)^{-2} \times\left[\cos\theta - rL\left(\sigma_2\right)^{-2}\sin^2\theta\right], \tag{9a}$$

$$\partial^2 P_{12}(r,\theta)/\partial r\partial\theta = -P_{12}(r,\theta) \quad L(\sigma_2)^{-2}\sin\theta \times\left\{1 + rL(\sigma_2)^{-2}\cos\theta - r^2\left[(\sigma_1)^{-2}+(\sigma_2)^{-2}\right]\right\}, \tag{9b}$$

$$\partial^2 P_{12}(r,\theta)/\partial r^2 = -P_{12}(r,\theta)\left\{\left[(\sigma_1)^{-2}+(\sigma_2)^{-2}\right] - \left\{L(\sigma_2)^{-2}\cos\theta - r\left[(\sigma_1)^{-2}+(\sigma_2)^{-2}\right]\right\}^2\right\}. \tag{9c}$$

At the position of the extremum (8a,b), the second-order derivatives (9a,b,c) take the values:

$$\left\{\partial^2/\partial\theta^2, \partial^2/\partial\theta\partial r, \partial^2/\partial r^2\right\} P_{12} = -P_m\left\{r_m L/(\sigma_2)^2, 0, (\sigma_1)^{-2}+(\sigma_2)^{-2}\right\}, \tag{10a,b,c}$$

where P_m is the value at the extremum:

$$P_m \equiv P_{12}(r_m,\theta_m) = \left[1/(2\pi\sigma_1\sigma_2)\right] \times\exp\left\{-(L^2/2)/\left[(\sigma_1)^2+(\sigma_2)^2\right]\right\}; \tag{11}$$

since:

$$d^2P_{12} = P_m \times\left\{r_m L(\sigma_2)^{-2}(d\sigma)^2 + \left[(\sigma_1)^{-2}+(\sigma)^{-2}\right](dr)^2\right\}, \tag{12}$$

is negative for arbitrary $d\sigma$ and dr, the extremum is actually a maximum. The maximum probability of coincidence (11) is given per unit of distance squared, i.e. per distance flown by each aircraft. Since the ICAO TLS specifies a probability of collision per distance (or flight hour) flown, it is necessary to integrate over all possible positions coincidence is possible anywhere, and thus integrating over all space specifies a three-dimensional cumulative probability of coincidence.

3 Three-dimensional cumulative probability of coincidence

The cumulative probability of coincidence over all space is given :

$$\overline{\overline{P}} \equiv \int_0^{2\pi} d\phi \int_0^{\pi} d\theta \int_0^{\infty} dr\, P_{12}(r,\theta)\, r^2 \sin\theta, \tag{13}$$

using the collision probability (5) in spherical coordinates (*Figure 2*):

$$\overline{\overline{P}} = \left[1/(\sigma_1\sigma_2)\right]\exp\left\{\left[-(L/\sigma_2)^2\right]/2\right\} \times\int_0^{\infty} r^2 I_0(r)\left\{\exp-(r^2/2)\left[(\sigma_1)^{-2}+(\sigma_2)^{-2}\right]\right\} dr. \tag{14}$$

where the $d\phi$-integration in (13) is trivial, and the $d\theta$-integration appears in:

$$I_0(r) \equiv \int_0^{\pi} \exp\left[rL(\sigma_2)^{-2}\cos\theta\right]\sin\theta\, d\theta. \tag{15}$$

This integral is elementary:

$$I_0(r) = -\left[(\sigma_2)^2/rL\right]\exp\left[rL(\sigma_2)^{-2}\cos\theta\right]_0^{\pi}, \tag{16}$$

so that only the dr-integration remains in (14). Substituting (16) in (14), the three-dimensional cumulative probability of collision is given by:

$$\overline{\overline{P}} = (\sigma_2/\sigma_1)L^{-1}\exp\left[-(L/\sigma_2)^2/2\right] \quad (I_+ - I_-), \tag{17}$$

where $I_\pm$ are the dr-integrations:

$$I_\pm \equiv \int_0^{\infty} r \quad \exp\left[-(r^2/2)(\sigma_1^{-2}+\sigma_2^{-2}) \pm rL\,\sigma_2^{-2}\right] dr. \tag{18a}$$

The change of variable $r \to -r$:

$$I_\pm = \int_0^{-\infty} r\exp\left[-(r^2/2)(\sigma_1^{-2}+\sigma_2^{-2}) \mp rL\sigma_2^{-2}\right] dr, \tag{18b}$$

shows that:

$$I_+ - I_- = \int_{-\infty}^{+\infty} r\exp\left[-(r^2/2)(\sigma_1^{-2}+\sigma_2^{-2}) + rL\sigma_2^{-2}\right] dr, \tag{19}$$

so that it is sufficient to evaluate this integral. The latter is reducible to the well-known Gaussian integral:

$$\int_{-\infty}^{+\infty} \exp(-\zeta^2)\, d\zeta = \sqrt{\pi}, \tag{20}$$

as will be shown next.

The change of variable:

$$\zeta \equiv \left(r/\sqrt{2}\right)(\sigma_1^{-2}+\sigma_2^{-2})^{1/2} - \xi, \quad \xi \equiv \left(L/\sqrt{2}\right)\sigma_2^{-2}\left(\sigma_1^{-2}+\sigma_1^{-2}\right)^{-1/2}, \tag{21a,b}$$

where the ξ is a constant, implies:

$$dr = \sqrt{2}\left(\sigma_1^{-2}+\sigma_2^{-2}\right)^{-1/2} d\zeta, \quad -(r^2/2)(\sigma_1^{-2}+\sigma_2^{-2}) + rL\sigma_2^{-2} = -\zeta^2 + \xi^2; \tag{22a,b}$$

substitution of (22a,b) in (19) yields.

$$I_+ - I_- = 2\left(\sigma_1^{-2}+\sigma_2^{-2}\right)^{-1}$$
$$\times \exp\left(\xi^2\right)\int_{-\infty}^{+\infty}\left(\zeta+\xi\right)\exp\left(-\zeta^2\right)d\zeta\,, \qquad (23a)$$

where: (i) the first term is zero, because the integrand $\zeta \exp\left(-\zeta^2\right)$ is an odd function of ζ integrated over the real line; (ii) the second term is specified by the Gaussian integral (20), *viz.*:

$$I_+ - I_- = 2\sqrt{\pi}\left(\sigma_1^{-2}+\sigma_2^{-2}\right)^{-1}\xi \quad \exp\left(\xi^2\right)$$
$$= \sqrt{2\pi}\;\; L\left(\sigma_2\right)^{-2}\left(\sigma_1^{-2}+\sigma_2^{-2}\right)^{-3/2}$$
$$\times \exp\left[\left(L^2/2\right)\sigma_2^{-4}/\left(\sigma_1^{-2}+\sigma_2^{-2}\right)\right], \qquad (23b)$$

where (21b) was used. Substitution of (23b) in (17) specifies the three-dimensional cumulative probability of coincidence:

$$\bar{\bar{P}} = \sqrt{2\pi}\left(\sigma_1\sigma_2\right)^2\left[\left(\sigma_1\right)^2+\left(\sigma_2\right)^2\right]^{-3/2}$$
$$\times \exp\left\{-\left(L^2/2\right)/\left[\left(\sigma_1\right)^2+\left(\sigma_2\right)^2\right]\right\}. \qquad (24)$$

Note that this is a probability of coincidence times distance flown, because it results from the integration in three dimensions of a probability of coincidence per square of distance flown. Thus it does not have the dimension of the ICAO TLS, of probability of coincidence per distance flown. The latter will result if the probability of coincidence per square of distance flown is integrated in one dimension, e.g. along the flight path.

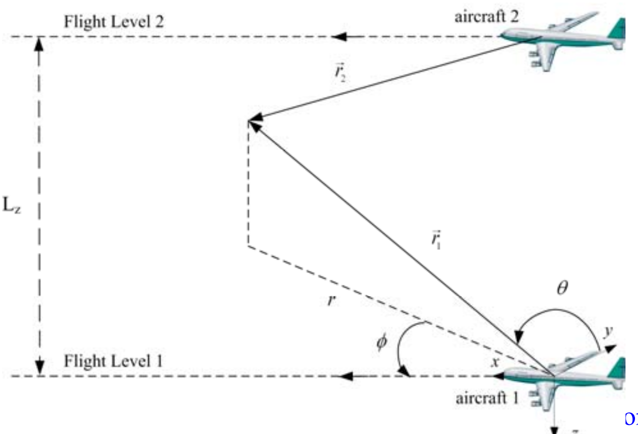

on aircraft one, and polar axis along the flight path, the probability of coincidence depends on (r, θ) but not on φ, because the configuration is axisymetric around the flight path.

4 Cumulative probability of coincidence along the flight path

The probability of coincidence along the flight path is obtained by setting θ = 0 in (5), viz:

$$P_{12}\left(r,0\right) = \left[1/\left(2\pi\sigma_1\sigma_2\right)\right]\exp\left[-\left(L/\sigma_2\right)^2/2\right]$$
$$\times \exp\left[-\left(\,r^2/2\right)\left(\sigma_1^{-2}+\sigma_2^{-2}\right)+rL\sigma_2^{-2}\,\right]. \qquad (25a)$$

The cumulative probability of coincidence along the flight path is obtained by a single dr-integration over the real line:

$$\bar{P} \equiv \int_{-\infty}^{+\infty} P_{12}\left(r,0\right)dr\,, \qquad (25b)$$

and is thus specified by evaluation of the integral

$$\bar{P} = \left[1/\left(2\pi\sigma_1\sigma_2\right)\right]\quad \exp\left[-\left(L/\sigma_2\right)^2/2\right]$$
$$\times\int_{-\infty}^{+\infty}\exp\left[-\left(r^2/2\right)\left(\sigma_1^{-2}+\sigma_2^{-2}\right)+rL\sigma_2^{-2}\right]dr\,; \qquad (26)$$

use of the same change of variable (21a,b) leads as before (22a,b) to:

$$\bar{P} = \left[\;1/\left(\sqrt{2}\,\pi\sigma_1\sigma_2\right)\;\right]\left(\sigma_1^{-2}+\sigma_2^{-2}\right)^{-1/2}$$
$$\times\exp\left[\;-\left(L/\sigma_2\right)^2/2\right]\exp\left(\xi^2\right)\int_{-\infty}^{+\infty}\exp\left(-\zeta^2\right)\;d\zeta\,; \qquad (27)$$

using the Gaussian integral (20), and substituting (21b) simplifies (27) to

$$\bar{P} = \left[\;1/\left(\sqrt{2\pi}\;\right)\right]\left[\;\left(\sigma_1\right)^2+\left(\sigma_2\right)^2\;\right]^{-1/2}$$
$$\times\exp\left\{\;-\left(L^2/2\right)/\left[\;\left(\sigma_1\right)^2+\left(\sigma_2\right)^2\;\right]\right\} \qquad (28)$$

which is the final expression for the one-dimensional cumulative probability of coincidence along the flight path.

In the case of aircraft with identical r.m.s. position errors, (28) simplifies to:

$$\bar{P} = \left[\;1/\left(2\sigma\sqrt{\pi}\;\right)\right]\quad\exp\left\{-\left[\;L/\left(2\sigma\right)\;\right]^2\right\}. \qquad (29)$$

In the general case (2b) of aircraft with dissimilar r.m.s. position errors σ_1 and σ_2, or variances $(\sigma_1)^2$ and $(\sigma_2)^2$, the arithmetic mean:

$$2\bar{\sigma}^2 \equiv (\sigma_1)^2 + (\sigma_2)^2, \tag{30a}$$

appears in (28):

$$\bar{P} = \left[1/\left(2\bar{\sigma}\sqrt{\pi}\right)\right]\exp\left\{-\left[L/(2\bar{\sigma})\right]^2\right\}, \tag{30b}$$

instead of σ in (29). The maximum probability of collision (11) simplifies, for aircraft with identical r.m.s. position errors, to:

$$P_m = \left[1/\left(2\pi\sigma^2\right)\right] \quad \exp\left\{-\left[L/(2\sigma)\right]^2\right\}. \tag{31}$$

In the general case of aircraft with dissimilar r.m.s. position errors σ_1 and σ_2, or variances $(\sigma_1)^2$ and $(\sigma_2)^2$, the maximum probability of coincidence (11), involves not only the arithmetic mean of variances (30a), but also the geometric mean of variances:

$$\sigma_1\sigma_2 = \sqrt{(\sigma_1)^2(\sigma_2)^2} \equiv \bar{\sigma}^2/f, \tag{32a}$$

and thus can be written in the form:

$$P_m = f\left[1/\left(2\pi\bar{\sigma}^2\right)\right]\exp\left\{-\left[L/(2\bar{\sigma})\right]^2\right\}, \tag{32b}$$

where f is a dimensionless factor.

The function f defined by (32a) is the ratio of the arithmetic (30a) to the geometric mean of variances:

$$f = \left[(\sigma_1)^2 + (\sigma_2)^2\right]/(2\sigma_1\sigma_2) = (\sigma_1/\sigma_2 + \sigma_2/\sigma_1)/2, \tag{33a}$$

and may be called the dissimilarity factor, since in general it depends only on the ratio of r.m.s. position errors:

$$f(\lambda) = (\lambda + 1/\lambda)/2 = f(1/\lambda), \lambda \equiv \sigma_1/\sigma_2, \tag{33b,c}$$

and in particular case of identical aircraft reduces to unity which is its minimum value for all λ:

$$\sigma_1 = \sigma_2 = \sigma: \quad \lambda = 1, \quad f(\lambda) \geq f_{\min} = f(1) = 1. \tag{34a,b}$$

The three-dimensional probability of coincidence (24) simplifies for aircraft with identical r.m.s. position errors to:

$$\sigma_1 = \sigma_2 \equiv \sigma: \quad \bar{\bar{P}} = \left(\sigma\sqrt{\pi}/2\right)\exp\left\{-\left[L/(2\sigma)\right]^2\right\}. \tag{35}$$

In the general case (24) of aircraft with dissimilar r.m.s. position errors, using the arithmetic (30a) and geometric (32a) means of variances, leads to:

$$\bar{\bar{P}} = \left(\sqrt{\pi}/2\right)\left(\bar{\sigma}/f^2\right)\exp\left\{-\left[L/(2\bar{\sigma})^2\right]\right\}. \tag{36}$$

In conclusion: (i) the maximum P_m, one-dimensional $\bar{P}$ and three-dimensional $\bar{\bar{P}}$ probabilities of coincidence all feature the exponential term $\exp\left\{-\left[L/(2\sigma)\right]^2\right\}$ for identical aircraft, respectively in (31; 29; 35); (ii) in the case of aircraft with dissimilar r.m.s. position errors σ is replaced in the exponential term $\exp\left\{-\left[L/(2\bar{\sigma})\right]^2\right\}$, respectively in (32b; 30b; 36), by $\bar{\sigma}$ defined from (30a) the geometric mean of variances; (iii) in the case of the one-dimensional cumulative probability of collision along the flight path $\bar{P}$, the factor multiplying the exponential in (30b), involves only the arithmetic mean of variances (30a); (iv) the geometric mean of variances (32a), appears through the dissimilarity function (33a, b, c), in the factor of the exponential in (32b) and (36), respectively for the maximum probability of coincidence P_m and the three-dimensional cumulative probability of coincidence $\bar{\bar{P}}$

5 Application to vertical separation at higher flight levels

Taking the general case of two aircraft with arbitrary or dissimilar r.m.s. position errors, three results have been obtained in the present paper: (i) the one-dimensional cumulative probability of coincidence (30b) along the flight path:

$$\bar{P} = 0.282095\,\bar{\sigma}^{-1}\exp\left[-0.25\left(L/\bar{\sigma}\right)^2\right]; \tag{45}$$

(ii) the maximum probability of coincidence (32b), which occurs vat the position (8a, b):

$$P_m = 0.159155\left(f/\bar{\sigma}^2\right)\exp\left[-0.25\left(L/\bar{\sigma}\right)^2\right]; \tag{46}$$

(iii) the three-dimensional cumulative probability of coincidence (36) over all space:

$$\bar{\bar{P}} = 0.886227\left(\bar{\sigma}/f^2\right)\exp\left[-0.25\left(L/\bar{\sigma}\right)^2\right]. \tag{47}$$

The last two expressions (46, 47) involve the aircraft dissimilarity function (33a, b, c).

Table I - Aircraft dissimilarity function and factor.

$\lambda \equiv \sigma_1/\sigma_2$	1	3	9
$f(\lambda)$	1	5/3	41/9
$1/\lambda = \sigma_2/\sigma_1$	1	1/3	1/9

The Table I confirms that the aircraft dissimilarity function is unchanged $f(\lambda)=f(1/\lambda)$ interchanging the two aircraft, i.e. exchanging σ_1 and σ_2, or λ and $1/\lambda$. Thus all three probabilities of coincidence (45,46,47) are unaffected by interchange of the two aircraft. Note that aircraft dynamics has been taken into account in the calculations; dynamics would limit the possible collisions, and thus the probabilities given here are uppers bounds.

As an example of application to ATM, the vertical separation of L= 2000ft = 0.329nm is considered, as specified by ICAO for higher flight levels. It is assumed that these altitudes are not limited either by ground obstructions or the service ceiling of the aircraft. This leads to the following probabilities of coincidence: (i) one-dimensional cumulative (45), per nautical mile flown:

$$L_a = 2000\text{ft}: \quad \bar{P}_a = 0.282\,\bar{\sigma}^{-1} \exp\left(-2.705\times10^{-2}/\bar{\sigma}^2\right), \tag{41a}$$

$$L_b = 1000\text{ft}: \quad \bar{P}_b = 0.282\,\bar{\sigma}^{-1} \exp\left(-6.763\times10^{-3}/\bar{\sigma}^2\right); \tag{41b}$$

(ii) maximum (46), per square nautical mile flown:

$$L_a = 2000\text{ft}: \quad P_{ma} = 0.159\left(f/\bar{\sigma}^2\right) \exp\left(-2.705\times10^{-2}/\bar{\sigma}^2\right), \tag{42a}$$

$$L_b = 1000\text{ft}: \quad P_{mb} = 0.159\left(f/\bar{\sigma}^2\right) \exp\left(-6.763\times10^{-3}/\bar{\sigma}^2\right); \tag{42b}$$

(iii) three-dimensional cumulative (47), times nautical miles flown:.

$$L_a = 2000\text{ft}: \quad \bar{\bar{P}}_a = 0.886\left(\bar{\sigma}/f^2\right) \exp\left(-2.705\times10^{-2}/\bar{\sigma}^2\right), \tag{43a}$$

$$L_b = 1000\text{ft}: \quad \bar{\bar{P}}_b = 0.886\left(\bar{\sigma}/f^2\right) \exp\left(-6.763\times10^{-3}/\bar{\sigma}^2\right). \tag{43b}$$

It has been found before in other applications [5] that the ICAO target level of safety (52a):

$$S = 5\times10^{-9}h^{-1}, \quad L/\sigma \sim 10-12, \tag{52a,b}$$

is obtained for r.m.s. position error about one order-of-magnitude less than the minimum separation distance. Since L=2000ft this suggests considering values of $\bar{\sigma}$ around 200ft, below and above up to less than L, in Table II.

The ICAO TLS (52a) can be applied to the one-dimensional cumulative probability of coincidence, e.g. $\bar{P} = 3.76\times10^{-13}$ per nautical mile for $\bar{\sigma} = 180$ ft from Table II. The probability of coincidence per hour flown $\bar{P}V \le S$ does not exceed the ICAO TLS standard for speeds $V \le S/\bar{P} = 1.33\times10^4 kt$, which includes all existing aircraft; for a great circle tour of the earth $D = 4\times10^4 km = 2.16\times10^4 nm$, the probability of coincidence would not exceed $\bar{P}D = 8.12\times10^{-9}$. Concerning the maximum probability of coincidence, from Table II it is $P_m = 2.49\times10^{-15}$ per nautical mile squared for $\bar{\sigma} = 160$ ft. The modified ICAO TLS standard $R = 5\times10^{-9}$ per hour squared would be satisfied $R \ge P_m V^2$, for speeds up to $V \le \sqrt{R/P_m} = 1.42\times10^3 kt$, which covers all current aircraft, including Concorde; for an aircraft dissimilarity factor λ=3 or 9, the maximum probability of coincidence would increase to $P_m = 4.15\times10^{-15}$ and 1.13×10^{-14}, and the modified ICAO TLS standard would be satisfied for speeds up to $V \le 1.10\times10^3 kt$ and $V \le 6.65\times10^2 kt$ which include all subsonic transports. For a great circle tour of the earth, the maximum probability of coincidence would be $P_m D^2 = (1.16, 1.93, 5.27)\times10^{-6}$ respectively in the cases λ=1, 3, 9. The three-dimensional cumulative probability of coincidence is $\bar{\bar{P}} = 1.13\times10^{-4}$ times nautical mile for $\bar{\sigma} = 400\,ft$ for $\lambda = 5$ in Table II. A modified ICAO TLS standard $\bar{Q} = 5\times10^{-9}$ times hour would be satisfied $\bar{Q} \le \bar{\bar{P}}/V$ for velocities up to $V \le \bar{\bar{P}}/\bar{Q} = 2.26\times10^4 kt$; for λ=3,9 the corresponding values $\overline{\overline{P}} = 4.07\times10^{-5}$, $1.96\times10^{-6}\,nm$ would be $V \le 8.14\times10^{3}$, $3.92\times10^{2}\,kt$. The three-dimensional probability of collision for a great circle tour of the earth would be $\overline{\overline{P}}/D = 5.23\times10^{-9}$, 1.88×10^{-9}, 9.08×10^{-11} respectively for λ=1, 3, 9.

6 Discussion

The ICAO target level of safety specifies a probability of collision $S = 5\times10^{-9}$ per hour flown, which may be converted into: (i) probability of collision *S*/*V* per nautical mile flown at a speed *V* in knots; (ii) probability of collision *S*.*T* for a flight of duration *T* in hours; (iii) probability of collision *S*.*D*/*V* for a flight at speed *V* knots over a distance *D* in nautical miles. The ICAO TLS is applicable to the one-dimensional cumulative probability of coincidence, which is (45) a probability of coincidence per unit of distance flown; the unit of distance, e.g. nautical mile, should be the same for the separation distance *L* and r.m.s. position error $\overline{\sigma}$, calculated from (30a) the arithmetic mean of variances of the position errors of the two aircraft.

When using the maximum probability of coincidence (46) the latter appears as per square of the distance flown. In the examples a modified ICAO TLS level $R = 5\times10^{-9}$ per hour flown squared was used; this value is more restrictive than the original ICAO TLS standard $S = 5\times10^{-9}$ per hour flown, in that it specifies a smaller position error $\overline{\sigma}$. However, it is not necessary to specify the same value 5×10^{-9} for *R*; another value could change the conclusion concerning $\overline{\sigma}$. In contrast, the three-dimensional probability of coincidence (47) is specified times distance flown; a modified ICAO TLS standard $Q = 5\times10^{-9}$ times hour, is a less severe restriction, in that it leads to larger r.m.s. position error $\overline{\sigma}$. The conclusion could be changed for another value of *Q*, thus there remains the open question of whether the original ICAO TLS standard 5×10^{-9} per hour, which is suitable for the cumulative probability of collision, should be supplement by two additional modified standards: (i) one per hour flown squared, suitable for comparison with maximum probabilities of collision; (ii) another times hour flown, for comparison with three-dimensional probabilities of collision. All of these could be used as alternative or complementary safety metrics.

References

[1] Eurocontrol. *Objective measures of ATM system safety: safety metrics*. CARE-INTEGRA Report to Eurocontrol, Brussels, Jan. 2000.

[2] Eurocontrol. *Air Traffic Management strategy for 2000+*. 2003.

[3] Barnett, A. Free flight and en route air safety a first-order analysis. *Operations Research*, Vol. 48, Nº6, pp. 833-845, 2000.

[4] ICAO. Rules of the air and air traffic services. 13th ed., Montreal, Canada, 1996.

[5] Ballin, M. G., Wing, D. J., Hughes, M.F. and Conway, S.R. Airborne separation assurance and air traffic management: research and concepts and technology, AIAA Paper 99-3, 1999.

[6] Anderson, E.W. *Principles of Navigation*. Hollis and Carter. 1966.

[7] Leighton, S.J., McGregor, A.E., Lowe, D., Wolfe, A. and Macaulay, A.A. GNSS guidance for all phases of flight: practical results. *Journal of Navigation*, Vol. 54, pp. 1-13, 1994.

[8] Tomlin, C., Pappas, J. and Sastry, S. Conflict resolution in air traffic management: a study in multi-agent hybrid systems. *IEEE Transactions on Automatic Control*, Vol. 43, Nº4,pp. 509-521, 1998.

[9] Reich, P.G. Analysis of long-range air traffic systems: separation standards. *Journal of Royal Institute of Navigation*, Vol. 19, pp. 88-98, pp. 169-186, pp. 331-347, 1972.

[10] Eurocontrol. European studies of vertical separation above FL290 - Summary report, Brussels, Oct., 1998.

[11] Harisson, D. and Moek, G. European studies to investigate the feasibility of using 1000 ft vertical separation minima above FL 290: Part I: Overview of organization, techniques employed and conclusions. *Journal of Navigation*, Vol. 44, 1992, pp. 171, 1992.

[12] Cox, M.E., ten Have, J.M. and Forrester, D.A. European studies to investigate the feasibility of using 1000 ft vertical separation minima above FL 290: Part II: Precision data analysis and collision risk assessment. *Journal of Navigation*, Vol. 45, pp. 91, 1992.

[13] Moek, G., ten Have, J.M., Harisson, D. and Cox, M.E. European studies to investigate the feasibility of using 1000 ft vertical separation minima above FL

290: Part III: Overview of organization, techniques employed and conclusions. *Journal of Navigation*, Vol. 46, pp. 245, 1992.

[14] Campos, L.M.B.C. On the probability of collision between aircraft with dissimilar position errors. *Journal of Aircraft*, Vol. 38, pp. 593-599, 2001.

[15] Campos, L.M.B.C. and Marques, J.M.G. On safety metrics related to aircraft separation. *Journal of Navigation*, Vol. 55, pp. 39-63, 2002.

[16] Shortie, J.F., Xie, Y., Chen, C.H. and Dunohue, G.L. Simulating Collision Probabilities of Landing Airplanes at Non-Towered Airports. *Simulation*, Vol. 80, pp. 21-31, 2004.

[17] Houck, S. and Powell, J.D. Assessment of probability of mid-air collision during an ultra closely spaced parallel approach, AIAA Paper 2001-4205, 2001.

[18] Etkin, B. The turbulent wind and its effects on flight. *Journal of Aircraft*, Vol. 18, Nº5, 1981.

[19] Etkin, B. and Etkin, D.A. Critical aspect of trajectory prediction flight in a non-uniform wind. *Agardograph AG-301*, Vol. 1, 1990.

[20] Campos, L.M.B.C. On the influence of atmospheric disturbances on aircraft aerodynamics. *Aeronautical Journal*, June/July, pp. 257-264, 1984.

[21] Campos, L.M.B.C. On the aircraft flight performance in a perturbed atmosphere. *Aeronautical Journal*, Oct., pp. 301-312, 1986.

[22] Campos, L.M.B.C. On a pitch control low for constant glide slope through wind shears and other disturbances. *Aeronautical Journal*, Sept., pp. 290-300, 1989.

[23] Etkin, B. and Reid, L.D. *Dynamics of flight: Stability and Control.* Wiley, 1996.

[24] Campos, L.M.B.C. and Aguiar, A.J.M N. On the inverse phugoid problem as an instance of non-linear stability in pitch. *Aeronautical Journal*, Oct. pp. 241-253, 1989.

[25] Campos, L.M.B.C., Fonseca, A.A. and Azinheira. Some elementary aspects of non-linear airplane speed stability in constrained flight. *Progress in Aerospace Sciences*, Vol. 31, pp. 137-169, 1995.

[26] Campos, L.M.B.C. On the non-linear longitudinal stability of symmetrical aircraft. *Journal of Aircraft*, Vol. 36, pp. 360-369, 1997.

[27] Campos, L.M.B.C. and Marques, J.M.G. On wake vortex response for all combinations of five classes of aircraft. *Aeronautical Journal*, June, pp. 295-310, 2004.

[28] Mises, R.V. *Theory of probability and statistics*. Academic Press, 1960.

[29] Lindeberg, J.W. Ueber der exponential gezetzes in der Wahrlicheinkalkulus. *Zeitschrift fur Mathematik*, Vol. 15, pp. 211-225, 1922.

[30] Reiss, R.D. and Thomas, M. *Statistical analysis of extreme values*. Birkhauser Verlag, 2001.

[31] Johnson, N.L. and Balakrishnan, N. *Continuous univariate probability distributions.* New York, Wiley, 1995.

[32] Campos, L.M.B.C. and Marques, J.M.G. On the combination of the Gamma and generalized error distribution with application to aircraft flight path deviation. *Communications in Statistics- Theory and Methods*, Vol. 33, Nº10, pp. 2307-2332, 2004.

[33] Braff, R. and Shively, C. A method of over bounding ground based augmentation system heavy tail error distribution. *Journal of Navigation*, Vol. 58, pp. 83-103, 2005.

[34] Kozubowski, T.J. and Podgórsi, K. Asymmetric Laplace laws and modelling of financial data. *Mathematical and Computer Modelling*, Vol. 34, pp. 1003-1021, 2001.

[35] Jammalamadaka, S.R. and Kozubowski, T.J. New families of wrapped distributions for modelling skew circular data. *Communications in Statistics- Theory and Methods*, Vol. 33, Nº9, pp. 2059-2074, 2004.

[36] Campos, L.M.B.C. and Marques, J.M.G. On the probability of collision between climbing and descending aircraft. *Journal of Aircraft*, Vol. 44, Nº2, pp. 550-557, 2007.

[37] Campos, L.M.B.C. and Marques, J.M.G. On alternative safety metrics for the probability of the collision between aircraft. *In Progress in Industrial Mathematics at ECMI 2008*. Ed. Fitt, A.D.; Norbury, J.; Ockendon, H.; Wilson, London: Springer-Verlag, pp. 753-758, 2010.

Copyright Statement

TABLE II - Upper bound to probabilities of collision assuming Gaussian probability distribution with vertical separation L_a = 2000 ft.

Arithmetic Mean of Variances $\bar{\sigma}$ (ft)	Maximum probability of coincidence P_{ma} (per square nm)			1-A cumulative probability of coincidence $\bar{P}_a$ (per nm)	Three-dimensional probability of coincidence $\bar{\bar{P}}_a$ (times nm)		
	$\lambda = 9, 1/9$	$\lambda = 3, 1/3$	$\lambda = 1$		$\lambda = 1$	$\lambda = 3, 1/3$	$\lambda = 9, 1/9$
1000	9.85	3.60	2.16	6.31×10^{-1}	5.37×10^{-2}	1.93×10^{-2}	2.59×10^{-3}
500	1.96	7.17×10^{-1}	4.30×10^{-1}	6.28×10^{-2}	1.34×10^{-3}	4.80×10^{-4}	6.43×10^{-5}
400	3.23×10^{-1}	1.18×10^{-1}	7.09×10^{-2}	8.27×10^{-3}	1.13×10^{-4}	4.05×10^{-5}	5.43×10^{-6}
300	4.44×10^{-3}	1.63×10^{-3}	9.76×10^{-4}	8.54×10^{-5}	6.54×10^{-7}	2.35×10^{-7}	3.15×10^{-8}
200	9.29×10^{-9}	3.40×10^{-9}	2.04×10^{-9}	1.19×10^{-10}	4.05×10^{-13}	1.46×10^{-13}	1.95×10^{-14}
180	3.26×10^{-11}	1.19×10^{-11}	7.15×10^{-12}	3.75×10^{-13}	1.04×10^{-15}	3.73×10^{-16}	4.99×10^{-17}
160	1.13×10^{-14}	4.15×10^{-15}	2.49×10^{-15}	1.16×10^{-16}	2.53×10^{-19}	9.11×10^{-20}	1.22×10^{-20}
140	9.50×10^{-20}	3.47×10^{-20}	2.08×10^{-20}	8.51×10^{-22}	1.42×10^{-24}	5.11×10^{-25}	6.84×10^{-26}
120	1.29×10^{-27}	4.71×10^{-28}	2.83×10^{-28}	9.90×10^{-30}	1.21×10^{-32}	4.37×10^{-33}	5.84×10^{-34}
100	9.96×10^{-41}	3.64×10^{-41}	2.19×10^{-41}	6.38×10^{-43}	5.43×10^{-46}	1.95×10^{-46}	2.61×10^{-47}

TABLE III - Upper bound to probabilities of collision assuming Gaussian probability distribution with vertical separation L_b = 1000 ft.

Arithmetic Mean of Variances $\overline{\sigma}$ (ft)	Maximum probability of coincidence P_{mb} (per square nm)			1-A cumulative probability of coincidence $\overline{P}_b$ (per nm)	Three-dimensional probability of coincidence $\overline{\overline{P}}_b$ (times nm)		
	$\lambda = 9, 1/9$	$\lambda = 3, 1/3$	$\lambda = 1$		$\lambda = 1$	$\lambda = 3, 1/3$	$\lambda = 9, 1/9$
1000	20.85	7.63	4.58	1.33	1.14×10^{-1}	4.09×10^{-2}	5.47×10^{-3}
500	39.39	14.4	8.65	1.26	2.68×10^{-2}	9.66×10^{-3}	1.29×10^{-3}
400	35.07	12.83	7.70	8.98×10^{-1}	1.22×10^{-2}	4.40×10^{-3}	5.89×10^{-4}
300	18.49	6.77	4.06	3.55×10^{-1}	2.72×10^{-3}	9.79×10^{-4}	1.31×10^{-4}
200	1.29	4.73×10^{-1}	2.84×10^{-1}	1.65×10^{-2}	5.63×10^{-5}	2.03×10^{-5}	2.71×10^{-6}
180	3.68×10^{-1}	1.35×10^{-1}	8.08×10^{-2}	4.24×10^{-3}	1.17×10^{-5}	4.21×10^{-6}	5.64×10^{-7}
160	6.00×10^{-2}	2.20×10^{-2}	1.32×10^{-2}	6.15×10^{-4}	1.34×10^{-6}	4.82×10^{-7}	6.45×10^{-8}
140	3.94×10^{-2}	1.44×10^{-3}	8.66×10^{-4}	3.53×10^{-5}	5.90×10^{-8}	2.12×10^{-8}	2.84×10^{-9}
120	5.36×10^{-5}	1.96×10^{-5}	1.18×10^{-5}	4.12×10^{-7}	5.05×10^{-10}	1.82×10^{-10}	2.43×10^{-11}
100	3.72×10^{-8}	1.36×10^{-8}	8.16×10^{-9}	2.38×10^{-10}	2.03×10^{-13}	7.29×10^{-14}	9.76×10^{-15}